

Matter effects in long–baseline experiments, the flavor content of the heaviest (or lightest) neutrino and the sign of Δm^2

Paolo Lipari
I.N.F.N., sezione di Roma, and
Dipartimento di Fisica, Università di Roma “la Sapienza”,
P. A. Moro 2, I-00185 Roma, Italy

January 25, 2018

Abstract

The neutrinos of long baseline beams travel inside the Earth’s crust where the density is $\rho \simeq 2.8 \text{ g cm}^{-3}$. If electron neutrinos participate in the oscillations, matter effects will modify the oscillation probabilities with respect to the vacuum case. Depending on the sign of Δm^2 an MSW resonance will exist for neutrinos or anti–neutrinos with energy $E_\nu^{res} \simeq 4.7 \cdot |\Delta m^2| / (10^{-3} \text{ eV}^2) \text{ GeV}$. For Δm^2 in the interval indicated by the Super–Kamiokande experiment this energy range is important for the proposed long baseline experiments.

For positive Δm^2 the most important effects of matter are a 9% (25%) enhancement of the transition probability $P(\nu_\mu \rightarrow \nu_e)$ for the KEK to Kamioka (Fermilab to Minos and CERN to Gran Sasso) beam(s) in the energy region where the probability has its first maximum, and an approximately equal suppression of $P(\bar{\nu}_\mu \rightarrow \bar{\nu}_e)$. For negative Δm^2 the effects for neutrinos and anti–neutrinos are interchanged. Producing beams of neutrinos and antineutrinos and measuring the oscillation probabilities for both the $\nu_\mu \rightarrow \nu_e$ and $\bar{\nu}_\mu \rightarrow \bar{\nu}_e$ transitions can solve the sign ambiguity in the determination of Δm^2 .

1 Introduction

The data on atmospheric neutrinos collected by Super–Kamiokande [1, 2] and other detectors (Kamiokande, IMB, Soudan and MACRO [3, 4, 5, 6]) give good evidence for the existence of neutrino oscillations with $|\Delta m^2| \simeq 10^{-3}\text{--}10^{-2} \text{ eV}^2$. The experimental results show that the flux of muon (anti–)neutrinos is suppressed with respect to the standard–model prediction while the flux of electron (anti–)neutrinos is compatible with the no–oscillation prediction taking into account measurement errors and systematic

uncertainties. This suggests that the dominant effect of the oscillations is $\nu_\mu \rightarrow \nu_\tau$ transitions, in good agreement with the results of the Chooz experiment [10] that put strong limits on possible $\nu_e \rightarrow \nu_x$ transitions in the relevant region of L/E_ν .

It is possible that the observed disappearance of the muon (anti-)neutrinos is due to oscillation into a light sterile state [7], and also other forms of ‘new physics’ beyond the standard model have been proposed as explanations of the atmospheric neutrino data (see [8] for a critical discussion). In this work we will however only consider standard oscillations between three neutrino flavors. This is the simplest extension of the standard model that can describe the data, and can do it very successfully [1, 2]. In this framework one expects transitions between all flavors ($\nu_\mu \leftrightarrow \nu_\tau$, $\nu_\mu \leftrightarrow \nu_e$, $\nu_e \leftrightarrow \nu_\tau$), and a very important goal of future experiments will be the measurement of (or the setting of more stringent limits on) the transitions involving electron neutrinos.

Future experiments measuring the disappearance of reactor neutrinos with longer path-lengths (in particular the Kamland detector [9]) will be able to study $\nu_e \rightarrow \nu_x$ transitions down to lower values of Δm^2 , however, because of systematic uncertainties [10], it will be difficult to extend the sensitivity of reactor experiments to values of the mixing much lower than those already excluded by Chooz. Higher statistics measurement of the atmospheric neutrino fluxes have a good potential to search for the flavor transitions of the ν_e ’s [11, 12, 13] searching for up-down asymmetries in the e -like events. Also experiments [14] using long baseline (LBL) neutrino beams such as the KEK to Kamioka [15], Fermilab to Minos [16] and CERN to Gran Sasso [17] projects have a very interesting potential for measuring $\nu_\mu \rightarrow \nu_e$ transitions. The LBL beams are mostly composed of ν_μ ’s with a small ν_e contamination below the 1% level, and a detector with good electron identification capability, collecting a sufficiently large sample of events, can be sensitive to $\nu_\mu \rightarrow \nu_e$ transitions even for values of the mixing well below the Chooz limit.

Because of the sphericity of the earth, the neutrinos of LBL beams travel a few kilometers below the Earth’s surface, in a medium that can be considered as approximately homogeneous with an electron density $n_e \simeq 1.69 \cdot 10^{24} \text{ cm}^{-3}$ (corresponding to a density $\rho \simeq 2.8 \text{ g cm}^{-3}$ and an electron fraction $Y_e = n_e/(n_p + n_n) = 0.5$). If the electron neutrinos participate in the oscillations, the presence of matter modifies the oscillation probabilities. In this paper we will discuss in some detail the matter effects and their observable consequences.

The work is organized as follows: in the next section we introduce the theoretical framework used in this analysis (a single relevant Δm^2); in section 3 we discuss the existing limits on the three independent parameters present in this framework (Δm^2 and two mixing parameters); in section 4 we compute the neutrino effective squared masses and mixing matrix in matter; in section 5 we discuss the propagation of neutrinos in matter with a constant electron density (a good approximation for LBL beams); in section 6 we finally discuss the oscillation probabilities for LBL beams. A summary is given in section 7.

2 One mass scale approximation

In the general case of mixing between three neutrino flavors, one has to consider three masses m_1 , m_2 and m_3 , and a (3×3) unitary mixing matrix U that relates the flavor $\{|\nu_e\rangle, |\nu_\mu\rangle, |\nu_\tau\rangle\}$ and mass $\{|\nu_1\rangle, |\nu_2\rangle, |\nu_3\rangle\}$ eigenstates:

$$|\nu_\alpha\rangle = U_{\alpha j} |\nu_j\rangle \quad (1)$$

Without lack of generality we can label the mass eigenstates so that:

$$|m_3^2 - m_2^2| > |m_2^2 - m_1^2| \quad (2)$$

and

$$m_1^2 \leq m_2^2 \leq m_3^2 \quad \text{or} \quad m_1^2 \geq m_2^2 \geq m_3^2 \quad (3)$$

With this choice $|\nu_3\rangle$ is the ‘most isolated’ state separated by the largest mass difference gap from the neutrino closest in mass and is therefore the heaviest (or lightest) neutrino, correspondingly $|\nu_1\rangle$ is the lightest (or heaviest) neutrino state.

In this work we will make the approximation that a single mass scale is important for the experiments we are considering. More explicitly we will assume that:

1. the squared mass differences Δm_{12}^2 and Δm_{23}^2 are of different order of magnitude:

$$|m_3^2 - m_2^2| \gg |m_2^2 - m_1^2|, \quad (4)$$

2. the mass difference $|m_2^2 - m_1^2|$ is too small to give observable effects in the measurements considered.

The study of oscillations under these assumptions has been performed by several authors in the past [19, 20, 21]. Formally it corresponds to the study of neutrino oscillation under the hypothesis that two neutrinos are degenerate in mass ($m_2 \simeq m_1$). The use of the one mass scale approximation is motivated by three type of considerations:

1. Neutrino oscillations in this approximation can still produce transitions between all flavors, and therefore this is a much more general framework than the special case of two-flavor mixing. The description of oscillations remains however much simpler than in the general case, and therefore the one mass scale approximation represents a natural ‘minimum model’ to study oscillations.
2. In most theoretical models it is natural to expect that the squared mass differences are organized in a hierarchical form $|m_3^2 - m_2^2| \gg |m_2^2 - m_1^2|$.
3. Finally and most important, there are strong experimental indications, coming from experiments on solar neutrinos [22] that the mass difference Δm_{12}^2 controls the observed suppression of the solar neutrino fluxes, and is of order $\sim 10^{-5}$ eV² (for the MSW solutions) or $\sim 10^{-11}$ eV² (for the just-so solution). These low values of Δm_{12}^2 are unobservable in long-baseline experiments and can result in at most small

effects [23, 24] for low energy atmospheric neutrinos. Therefore if oscillations are the solution for both the atmospheric and the solar neutrino problems the one mass scale approximation is a completely adequate framework to describe long-baseline experiments, and is a reasonable model for the study of atmospheric neutrinos.

When two neutrinos are degenerate in mass the mixing matrix U is not completely defined. In fact the j -th column of the matrix $(U_{ej}, U_{\mu j}, U_{\tau j})$ describes the flavor content of the mass eigenstate $|\nu_j\rangle$, and the two states with the same mass $|\nu_1\rangle$ and $|\nu_2\rangle$ can be chosen in an infinite number of ways. The degeneracy is broken when neutrinos propagate in matter, because the ν_e and ν_μ (ν_τ) have different potentials (see next section), and in the subspace of the neutrino states orthogonal to $|\nu_3\rangle$ the states with and without a $|\nu_e\rangle$ component have different effective masses. It is therefore convenient to choose one of the eigenstates, for example the $|\nu_1\rangle$ state, as orthogonal to the flavor state $|\nu_e\rangle$, this also determines $|\nu_2\rangle$ (modulo some phase convention) as the normalized state orthogonal to $|\nu_1\rangle$ and $|\nu_3\rangle$. With these conventions the mixing matrix U can be parametrized as:

$$U = \begin{bmatrix} 0 & \cos\theta & \sin\theta \\ \cos\varphi & -\sin\theta\sin\varphi & \cos\theta\sin\varphi \\ -\sin\varphi & -\sin\theta\cos\varphi & \cos\theta\cos\varphi \end{bmatrix} \quad (5)$$

with the two mixing angles θ and φ defined in the interval $[0, \pi/2]$. The definition of the mixing matrix in equation (5) contains some arbitrary sign conventions (only the absolute values $|U_{\alpha j}|$ of the elements are uniquely defined), the important point is that it is possible to define all elements as real and all CP or T violating effects vanish in the one mass scale approximation. In the following we will also use the notation

$$p_{\alpha 3} = |\langle \nu_\alpha | \nu_3 \rangle|^2 = |U_{\alpha 3}|^2 \quad (6)$$

where $p_{\alpha 3}$ is the probability that the neutrino $|\nu_3\rangle$ has the flavor $|\nu_\alpha\rangle$. These probabilities obviously satisfy the relation:

$$p_{e3} + p_{\mu 3} + p_{\tau 3} = 1 \quad (7)$$

In the one mass scale approximation all oscillation effects (also in the presence of matter) can be expressed as a function of $\Delta m^2 = m_3^2 - m_1^2$ and of the three probabilities p_{e3} , $p_{\mu 3}$ and $p_{\tau 3}$. The transition probabilities in vacuum can be written as:

$$P_{\nu_\alpha \rightarrow \nu_\beta}^{vac}(L/E_\nu) = 4 p_{\alpha 3} p_{\beta 3} \sin^2 \left[\frac{\Delta m^2 L}{4 E_\nu} \right] \quad (8)$$

and the survival probabilities as:

$$P_{\nu_\alpha \rightarrow \nu_\alpha}^{vac}(L/E_\nu) = 1 - 4 p_{\alpha 3} (1 - p_{\alpha 3}) \sin^2 \left[\frac{\Delta m^2 L}{4 E_\nu} \right], \quad (9)$$

For fixed E_ν all probabilities oscillate with a single oscillation length $\lambda_0(E_\nu)$:

$$\lambda_0(E_\nu) = \frac{4\pi E_\nu}{|\Delta m^2|} \simeq 2.470 \frac{E_\nu(\text{GeV})}{\Delta m^2(\text{eV}^2)} \text{ km} \quad (10)$$

that grows linearly with increasing E_ν .

3 Experimental results

The available information on the oscillation probabilities in the region of interest are summarized in fig. 1 where we show the allowed regions obtained by the Super-Kamiokande (shaded area) and the Chooz experiment. The curves are taken from [2] and [10] where they were obtained in the framework of a two flavor oscillation analysis (we have only relabelled the x -axis as A_{ee} for Chooz limit and $A_{\mu\tau}$ for the SK result).

We want to translate these results into constraints on p_{e3} , $p_{\mu3}$ and $p_{\tau3}$. In the Chooz analysis the electron neutrino survival probability is described with the form $P_{\nu_e \rightarrow \nu_e} = 1 - A_{ee} \sin^2[\Delta m^2/4E_\nu]$, and an allowed region is determined for the parameters Δm^2 and A_{ee} . The form of the probability is identical to the one obtained in the framework of the one mass scale approximation, and using $A_{ee} = 4p_{e3}(1 - p_{e3})$ for any Δm^2 the allowed interval in A_{ee} can be translated in an allowed interval on p_{e3} (composed of two disconnected sub-intervals).

The SK analysis is valid only in the framework of two flavor ($\nu_\mu \leftrightarrow \nu_\tau$) oscillations, since it is assumed that the ν_e and $\bar{\nu}_e$ fluxes are not modified. In the framework of the one mass scale approximation, this corresponds to the limit $p_{e3} = 0$. In this limit, using $A_{\mu\tau} = 4 p_{\mu3} p_{\tau3}$, the allowed region in $A_{\mu\tau}$ can be translated in allowed intervals for $p_{\mu3}$ and $p_{\tau3}$. Since the Chooz results tell us that p_{e3} is small we can consider these intervals as a reasonable approximation. Taking into account the possibility of a non vanishing p_{e3} the allowed interval for $p_{\mu3}$ (or $p_{\tau3}$ is slightly enlarged (for a detailed discussion see [11]).

The results are shown in fig. 2. As an illustration of how to read the figure we can consider the value $|\Delta m^2| = 3 \times 10^{-3} \text{ eV}^2$. For this value of the squared mass difference the Chooz upper limit ($A_{ee} \leq 0.13$) tells us that the state $|\nu_3\rangle$ is either a quasi pure electron neutrino state or contains only a small overlap with $|\nu_e\rangle$:

$$p_{e3} \leq 0.033 \quad \text{or} \quad p_{e3} \geq 0.966 \quad (11)$$

The SK results tell us that there are oscillations between ν_μ and ν_τ and the amplitude of the oscillations is close to unity ($A_{\mu\tau} \geq 0.86$). This can be translated as:

$$0.32 \leq p_{\mu3}, p_{\tau3} \leq 0.68 \quad (12)$$

Of course the three probabilities are constrained to satisfy $p_{e3} + p_{\mu3} + p_{\tau3} = 1$, therefore only the ‘small e -flavor’ interpretation of the Chooz data remains acceptable, and a large (small) $p_{\mu3}$ implies a small (large) $p_{\tau3}$. We note that the best fit of Super-Kamiokande ($\sin^2 2\theta_{\mu\tau} = 1$) corresponds to $p_{\mu3} = p_{\tau3} = \frac{1}{2}$ and $p_{e3} = 0$.

A central goal of future experiments will be to measure more accurately the flavor content of the neutrino state $|\nu_3\rangle$, and in particular to measure (or put a more stringent limit) to the overlap between the $|\nu_3\rangle$ and $|\nu_e\rangle$ states.

We note that, in analogy with the charged lepton and quark masses, it is ‘natural’ to expect that the state $|\nu_3\rangle$, that is experimentally determined to be a combination with approximately equal weights of muon and tau neutrinos and a small (or vanishing) $|\nu_e\rangle$ component, is the heaviest neutrino. This however is an assumption that could be

false, and that should be experimentally verified. No oscillation experiment in vacuum can solve this ambiguity, since the mass dependent oscillating term $\sin^2[\Delta m^2 L/(4E_\nu)]$ is invariant for a change of sign in Δm^2 . If however neutrinos are propagating in matter, measurements of flavor transitions can determine the sign of Δm^2 , that is determine if the state $|\nu_3\rangle$ is the heaviest or lightest neutrino.

4 Matter effects

When neutrinos propagate in matter the interactions with the medium results in a a flavor dependent effective potential V_α [18]. The difference in effective potential between electron neutrinos and (tau) muon (anti)-neutrinos is:

$$V = V_e - V_\mu = V_e - V_\tau = \pm\sqrt{2} G_F n_e \quad (13)$$

where n_e is the electron density of the medium, G_F is the Fermi constant and the plus (minus) sign applies to neutrinos (anti-neutrinos). Using the relation

$$E_\nu = \sqrt{p^2 + m^2} + V \simeq p + \frac{m^2}{2p} + V \quad (14)$$

the potential can be considered as a contribution $\delta m^2(\nu_e) = 2E_\nu V$ to the effective squared mass of ν_e 's. The neutrino effective squared mass eigenvalues M_j^2 and the mixing matrix in matter U_m can calculated solving the equation:

$$U \begin{bmatrix} m_1^2 & 0 & 0 \\ 0 & m_2^2 & 0 \\ 0 & 0 & m_3^2 \end{bmatrix} U^T + \begin{bmatrix} 2V E_\nu & 0 & 0 \\ 0 & 0 & 0 \\ 0 & 0 & 0 \end{bmatrix} = U_m \begin{bmatrix} M_1^2 & 0 & 0 \\ 0 & M_2^2 & 0 \\ 0 & 0 & M_3^2 \end{bmatrix} U_m^T \quad (15)$$

The columns of the matrix U_m give the flavor components of a new set of 'propagation eigenvectors' $\{|\nu_{1m}\rangle, |\nu_{2m}\rangle, |\nu_{3m}\rangle\}$ with well defined effective mass in matter.

The matrix diagonalization problem of equation (15) is very simple under the assumption $m_1^2 = m_2^2$ and has been discussed before by several authors [19, 11, 12]. The neutrino state $|\nu_1\rangle$ has been chosen (see previous section) as having no electron flavor component, and therefore is decoupled from all matter effects, and the problem is equivalent to the well known case of two flavor mixing. The effective mass eigenvalues and the mixing matrix can be written as a function of the adimensional quantity x :

$$x = \frac{2VE_\nu}{\Delta m^2} = \pm \frac{2\sqrt{2} G_F n_e E_\nu}{\Delta m^2} \simeq \pm 0.076 \frac{\rho(g\text{ cm}^{-3}) E_\nu(\text{GeV})}{\Delta m^2(10^{-3} \text{ eV}^2)} \quad (16)$$

the plus (minus) sign applies to ν 's ($\bar{\nu}$'s). For the numerical estimate in (16) we have also assumed an electron fraction $Y_e = 0.5$.

The effective squared mass eigenvalues are:

$$M_1^2 = m_1^2$$

$$\begin{aligned}
M_2^2 &= m_1^2 + \Delta m^2 \frac{1}{2} \left[1 + x - \sqrt{\sin^2 2\theta + (x - \cos 2\theta)^2} \right] \\
M_3^2 &= m_1^2 + \Delta m^2 \frac{1}{2} \left[1 + x + \sqrt{\sin^2 2\theta + (x - \cos 2\theta)^2} \right]
\end{aligned} \tag{17}$$

The mixing matrix in matter U_m has the same form as in the vacuum case:

$$U_m = \begin{bmatrix} 0 & \cos \theta_m(x) & \sin \theta_m(x) \\ \cos \varphi & -\sin \theta_m(x) \sin \varphi & \cos \theta_m(x) \sin \varphi \\ -\sin \varphi & -\sin \theta_m(x) \cos \varphi & \cos \theta_m(x) \cos \varphi \end{bmatrix} \tag{18}$$

but the angle θ_m is a function of the parameter x :

$$\sin \theta_m(x) = \frac{(x - \cos 2\theta) + \sqrt{\sin^2 2\theta + (x - \cos 2\theta)^2}}{\{[(x - \cos 2\theta) + \sqrt{\sin^2 2\theta + (x - \cos 2\theta)^2}]^2 + \sin^2 2\theta\}^{\frac{1}{2}}} \tag{19}$$

The resulting $\sin^2 2\theta_m(x)$ has the well known expression:

$$\sin^2 2\theta_m(x) = \frac{\sin^2 2\theta}{\sin^2 2\theta + (x - \cos 2\theta)^2} \tag{20}$$

Note that we have given explicitly the three mass eigenvalues (and not only the difference $M_3^2 - M_2^2$), and also $\sin \theta_m$ (and not only $\sin^2 2\theta_m$), because these quantities are needed to compute 3-flavor oscillations, as we will discuss in the following.

An illustration of the effect of matter on the masses and mixing of the neutrinos is shown in figures 3, 4, 5 and 6. For these figures we have assumed $\Delta m^2 = 3 \cdot 10^{-3} \text{ eV}^2$, a probability $p_{e3} = |U_{e3}|^2 \equiv \sin^2 \theta = 0.025$ (the specification of $U_{\mu 3}$ and $U_{\tau 3}$ is not necessary) and that the neutrinos (or anti-neutrinos) propagate in matter of constant density $\rho = 2.8 \text{ g cm}^{-3}$ (with electron fraction $Y_e = 1/2$). This last condition is a good approximation for neutrinos in LBL beams that travel few kilometers below the Earth's surface. In fig. 3 we show the neutrino effective mass eigenvalues M_j^2 (equation 17) plotted as a function of E_ν . Fig. 4 is the same but for antineutrinos. In fig. 5 (fig. 6) we show the values of $\sin^2 \theta_m$ ($\sin^2 2\theta_m$) (again plotted as a function of E_ν), the solid (dashed) lines refer to ν 's ($\bar{\nu}$'s).

Note that in matter the propagation eigenvectors $|\nu_{1m}\rangle \equiv |\nu_1\rangle$ and $|\nu_{2m}\rangle$ are not anymore degenerate, since the effective mass of $|\nu_1\rangle$ can be considered as constant while the effective squared mass of the state $|\nu_{2m}\rangle$ ($|\bar{\nu}_{2m}\rangle$) increases (decreases) with increasing $n_e E_\nu$.

Inspecting the equations that describe the effective masses and mixing in matter, we can notice that there are some special conditions:

1. The case $x = 0$ is simply the vacuum case: $M_j^2(0) = m_j^2$ and $\theta_m(0) = \theta$.
2. The case $x \rightarrow +\infty$ corresponds to the limit of very large density or very large E_ν for neutrinos (anti-neutrinos) if $\Delta m^2 > 0$ ($\Delta m^2 < 0$). In this situation the state $|\nu_{3m}\rangle$

becomes a pure $|\nu_e\rangle$ ($\theta_m \rightarrow \pi/2$) with a very large effective mass $M_3^2 \rightarrow \infty$, and decouples from the oscillations; the state $|\nu_{2m}\rangle$ asymptotically has the effective mass $M_2^2 \rightarrow m_1^2 + \Delta m^2 \cos^2 \theta$. Note that in this condition of very strong matter effects, the oscillations involving ν_e are completely suppressed, but $\nu_\mu \leftrightarrow \nu_\tau$ oscillations do occur with a maximum probability $4 \sin^2 \varphi \cos^2 \varphi$ larger than the vacuum one by a factor $(\cos^2 \theta)^{-1}$, and an effective Δm^2 smaller than the vacuum value by a factor $\cos^2 \theta$.

3. The case $x \rightarrow -\infty$ corresponds to the limit of very large density, or very large E_ν for anti-neutrinos (neutrinos) if $\Delta m^2 > 0$ ($\Delta m^2 < 0$). In this situation the state $|\nu_{2m}\rangle$ becomes a pure $|\nu_e\rangle$ ($\theta_m \rightarrow 0$) with effective mass $M_3^2 \rightarrow -\infty$; the state $|\nu_{3m}\rangle$ asymptotically gets the mass $M_3^2 \rightarrow m_1^2 + \Delta m^2 \cos^2 \theta$. This situation is experimentally undistinguishable from the previous case.
4. Finally we have the special case:

$$x = \cos 2\theta = 1 - 2 p_{e3} \quad (21)$$

This case can only happen for neutrinos (anti-neutrinos) if $\Delta m^2 > 0$ ($\Delta m^2 < 0$). It corresponds to the celebrated MSW [18] resonance. For a fixed electron density, the resonance happens at a value of the neutrino energy:

$$E_\nu^{res} = \frac{\Delta m^2 \cos 2\theta}{2V} = 4.7 \cos 2\theta \left(\frac{|\Delta m^2|}{10^{-3} \text{ eV}^2} \right) \left(\frac{2.8 \text{ g cm}^3}{\rho} \right) \left(\frac{0.5}{Y_e} \right) \text{ GeV} \quad (22)$$

At the resonance the mixing angle in matter is $\theta_m = 45^\circ$, the probability $P(\nu_e \rightarrow \nu_e)$ oscillates with amplitude $\sin^2 2\theta_m = 1$, while the probabilities $P(\nu_e \rightarrow \nu_\mu)$ and $P(\nu_e \rightarrow \nu_\tau)$ oscillate with amplitudes $\sin^2 \varphi$ and $\cos^2 \varphi$.

5 Propagation in matter of constant density

For neutrinos propagating in matter of a constant density the oscillation probabilities can be written in general as the superposition of three oscillating terms corresponding to the three effective squared mass differences:

$$P_{\nu_\alpha \rightarrow \nu_\beta}(L, E_\nu; x) = \sum_{j < k} A_{\alpha\beta}^{jk}(x) \sin^2 \left[\pi \frac{L}{\lambda_{jk}(x, E_\nu)} \right]. \quad (23)$$

The amplitudes of the oscillating terms are given by:

$$A_{\alpha\beta}^{jk}(x) = -4 U_{\alpha j}^m U_{\beta j}^m U_{\alpha k}^m U_{\beta k}^m \quad (24)$$

The three oscillation lengths are:

$$\lambda_{jk}(E_\nu, x) = \frac{4\pi E_\nu}{|M_j^2 - M_k^2|} \quad (25)$$

and satisfy the relation:

$$\lambda_{13}^{-1} - \lambda_{12}^{-1} - \lambda_{23}^{-1} = 0 \quad (26)$$

They can be written explicitly as a function of the parameter x :

$$\lambda_{12}(E_\nu, x) = \lambda_0(E_\nu) \left[\frac{1}{2} \left(1 + x - \sqrt{F(x)} \right) \right]^{-1} \quad (27)$$

$$\lambda_{13}(E_\nu, x) = \lambda_0(E_\nu) \left[\frac{1}{2} \left(1 + x + \sqrt{F(x)} \right) \right]^{-1} \quad (28)$$

$$\lambda_{23}(E_\nu, x) = \lambda_0(E_\nu) \left[\sqrt{F(x)} \right]^{-1} \quad (29)$$

where we have introduced the definition

$$F(x) = \sin^2 2\theta + (x - \cos 2\theta)^2 \quad (30)$$

In fig. 7 we show as an example a plot of the oscillation lengths λ_{jk} calculated as a function of the neutrino energy for the same values of the neutrino masses, and mixing and the same density of the medium as in the previous figures. Some features are immediately visible looking at fig. 7:

1. The presence of matter introduces an energy independent length:

$$\lambda_m(n_e) = \frac{2\pi}{|V|} = 1.16 \cdot 10^4 \text{ km} \left(\frac{1.69 \cdot 10^{24} \text{ cm}^{-3}}{n_e} \right) \quad (31)$$

2. When $x \rightarrow 0$ (low $n_e E_\nu$) we have $\lambda_{12} \rightarrow \lambda_m$, $\lambda_{13}, \lambda_{23} \rightarrow \lambda_0$. When $x \rightarrow \infty$ (high $n_e E_\nu$) we have $\lambda_{12} \rightarrow \lambda_0$, $\lambda_{13}, \lambda_{23} \rightarrow \lambda_m$.
3. The resonance condition can also be expressed as $\lambda_0(E_\nu) = \lambda_m(n_e) \cos 2\theta$. At the resonance the length λ_{23} has a maximum: $\lambda_{23} = \lambda_0 / \sin 2\theta$.

For a fixed value of E_ν the oscillation probabilities involving ν_e (or $\bar{\nu}_e$'s) have a simple sinusoidal dependence on L with oscillation length λ_{23} . This can be understood immediately observing that the eigenstate $|\nu_1\rangle$ has no electron flavor component. Formally we have that $U_{e1}^m = 0$, and therefore from (24) follows that:

$$A_{e\mu}^{12} = A_{e\mu}^{13} = A_{e\tau}^{12} = A_{e\tau}^{13} = 0 \quad (32)$$

therefore the transitions $\nu_e \leftrightarrow \nu_\mu$ and $\nu_e \leftrightarrow \nu_\tau$ develop with a single oscillation length λ_{23} . The probability $P(\nu_\mu \leftrightarrow \nu_\tau)$, and therefore also $P(\nu_\mu \rightarrow \nu_\tau)$, have a more complex functional form because all the three oscillating terms in (23) are non vanishing. The non vanishing probability amplitudes $A_{\alpha\beta}^{jk}$ can be written as:

$$\begin{aligned} A_{e\mu}^{23}(x) &= 4 \sin^2 \theta_m \cos^2 \theta_m \sin^2 \varphi &= \sin^2 2\theta_m \sin^2 \varphi \\ A_{e\tau}^{23}(x) &= 4 \sin^2 \theta_m \cos^2 \theta_m \cos^2 \varphi &= \sin^2 2\theta_m \cos^2 \varphi \\ A_{\mu\tau}^{23}(x) &= -4 \sin^2 \theta_m \cos^2 \theta_m \sin^2 \varphi \cos^2 \varphi &= -\sin^2 2\theta_m \sin^2 \varphi \cos^2 \varphi \\ A_{\mu\tau}^{12}(x) &= 4 \sin^2 \theta_m \sin^2 \varphi \cos^2 \varphi \\ A_{\mu\tau}^{13}(x) &= 4 \cos^2 \theta_m \sin^2 \varphi \cos^2 \varphi \end{aligned} \quad (33)$$

5.1 Small L regime

It is interesting to study the oscillation probabilities in matter in the limit of short neutrino pathlength L , or more precisely in the limit where $L/\lambda_{jk} \ll 1$ for all three oscillation lengths. The condition of ‘small L ’ is going to be valid in the range $E_\nu \gtrsim 10$ GeV for the long-baseline beams such as the Fermilab to Minos and CERN to Gran Sasso projects ($L \simeq 730$ km) if $|\Delta m^2|$ is in the range indicated by the atmospheric neutrino data.

In the limit of small L the oscillation probabilities in matter are undistinguishable from the vacuum case, even if the effective masses and mixing in matter are very different from the vacuum case. This can be demonstrated observing that when L/λ_{jk} is small the oscillating terms in (23) can be approximated as:

$$\sin^2\left(\pi \frac{L}{\lambda_{jk}}\right) \simeq \left(\pi \frac{L}{\lambda_{jk}}\right)^2 \quad (34)$$

and the oscillation probabilities take the form:

$$P_{\nu_\alpha \rightarrow \nu_\beta} = (\pi L)^2 \sum_{j < k} \frac{A_{\alpha\beta}^{jk}(x)}{\lambda_{jk}^2(E_\nu, x)} \quad (35)$$

There are now two relations between the amplitudes $A_{\alpha\beta}^{jk}$ and the oscillation lengths λ_{jk} that result in a cancellation of the x dependence of the expression (35). The first relation is present also in the case of two flavor mixing:

$$\frac{\sin^2 2\theta_m(x)}{\lambda_{23}^2(E_\nu, x)} = \left(\frac{\sin^2 2\theta}{F(x)}\right) \left(\frac{\sqrt{F(x)}}{\lambda_0(E_\nu)}\right)^2 = \frac{\sin^2 2\theta}{\lambda_0^2(E_\nu)} \quad (36)$$

where we have used equations (29) and (20) in the first equality. Similarly it is easy to prove that:

$$\frac{\sin^2 \theta_m}{\lambda_{12}^2} + \frac{\cos^2 \theta_m}{\lambda_{13}^2} = \frac{\cos^2 \theta}{\lambda_0^2}. \quad (37)$$

From equation (33) we can see that $A_{\alpha\beta}^{23} \propto \sin^2 2\theta_m$, $A_{\alpha\beta}^{12} \propto \sin^2 \theta_m$ and $A_{\alpha\beta}^{13} \propto \cos^2 \theta_m$, and using the relations (36) and (37) in (35) one can see that for L/λ_{jk} small the matter effects have no experimentally detectable effects.

To illustrate this point in fig. 8 and fig. 9 we show the transition probability $P(\nu_\mu \rightarrow \nu_e)$ and $P(\nu_\mu \rightarrow \nu_\tau)$ plotted as a function of the distance L for neutrinos and anti-neutrinos of a fixed energy $E_\nu = 13.0$ GeV traveling in vacuum or in matter of constant matter with density $\rho = 2.8$ g cm⁻³. For these figures we have assumed again for illustration $\Delta m^2 = 3 \cdot 10^{-3}$ eV², $p_{e3} = \sin^2 \theta = 0.025$ and $p_{\mu 3} = p_{\tau 3}$. The energy $E_\nu = 13.0$ GeV is close to the neutrino resonance energy (13.4 GeV) for the density and mass matrix considered. Note that the maximum pathlength considered in these plots $L = 5 \cdot 10^4$ km is approximately four times longer than the Earth’s diameter and therefore in most of the range of pathlengths considered the condition considered cannot be realized in practice.

Looking at the figure it is immediately evident that the oscillation properties of the neutrinos in matter and in vacuum are dramatically different, however experiments with a baseline of $L = 250$ or 730 km will not measure significant departures from the vacuum oscillation probabilities.

6 Oscillation probabilities for LBL experiments

In a LBL experiment the neutrino pathlength L and the electron density $n_e(y)$ along the trajectory ($y \in [0, L]$ is a coordinate along the neutrino path) can be considered as fixed, therefore what are experimentally accessible, are the oscillation probabilities $P_{\nu_\alpha \rightarrow \nu_\beta}(E_\nu)$ as function of the neutrino energy. In the following we will also use the approximation to consider n_e as constant.

If L and n_e are fixed, in the one mass scale approximation for a long baseline experiment one has to consider two characteristic neutrino energies:

$$\varepsilon_0 = \frac{|\Delta m^2| L}{2\pi} = 0.59 |\Delta m_{-3}^2| \left(\frac{L}{730 \text{ km}} \right) \text{ GeV} \quad (38)$$

and

$$\varepsilon_m = \frac{|\Delta m^2|}{2V} = \frac{|\Delta m^2|}{2\sqrt{2}G_f n_e} = 4.70 |\Delta m_{-3}^2| \left(\frac{1.69 \cdot 10^{24} \text{ cm}^{-3}}{n_e} \right) \text{ GeV} \quad (39)$$

where Δm_{-3}^2 is the value of the neutrino squared mass difference in units of 10^{-3} eV^2 . The energy ε_0 corresponds to the highest neutrino energy for which the vacuum transition probabilities have a maximum (or in different words it is the energy such that $\lambda_0(\varepsilon_0) = 2L$). The energy ε_m is the resonance energy in the limit of small p_{e3} :

$$E_\nu^{res} = \varepsilon_m \cos 2\theta = \varepsilon_m (1 - 2p_{e3}), \quad (40)$$

the parameter x that controls the importance of the matter effect is given by $|x| = E_\nu/\varepsilon_m$, and therefore for $E_\nu \ll \varepsilon_m$ the presence of matters has a negligible effect. Both characteristic energies are proportional to Δm^2 , and the ratio $\varepsilon_0/\varepsilon_m$ is independent from the neutrino mass matrix. For the Fermilab and CERN projects one has $\varepsilon_0/\varepsilon_m = 0.125$, for the KEK to Kamioka (K2K) project $\varepsilon_0/\varepsilon_m = 0.042$. The smallness of this ratio ensures that the matter effects are only a correction to the oscillation probabilities.

In fig. 10 and fig. 11 as an illustration we show the transition probabilities $P(\nu_\mu \rightarrow \nu_\tau)$ and $P(\nu_\mu \rightarrow \nu_e)$ plotted as a function of E_ν for neutrinos that have traveled the distance $L = 730$ km in vacuum (solid line) or in matter with constant density $\rho = 2.8 \text{ g cm}^{-3}$ (dashed line for neutrinos, dot-dashed line for antineutrinos). In these examples we have used $\Delta m^2 = 3 \cdot 10^{-3} \text{ eV}^2$, $p_{e3} = \sin^2 \theta = 0.025$, and $p_{\mu 3} = p_{\tau 3} = 0.4875$. The vacuum transition probabilities have a simple sinusoidal form:

$$P_{vac}(\nu_\alpha \rightarrow \nu_\beta) = A_{\alpha\beta} \sin^2 \left[\frac{\pi}{2} \frac{\varepsilon_0}{E_\nu} \right] \quad (41)$$

with maxima at $E_\nu = \varepsilon_0/n$ (n is a positive integer) where the probability has a value $A_{\alpha\beta} = 4p_{\alpha 3}p_{\beta 3}$. The presence of matter (for $p_{e3} \neq 0$) results in some deviations of the oscillation probabilities from the form (41). The effect, for $\Delta m^2 > 0$, is an enhancement (suppression) of the $\nu_\mu \rightarrow \nu_e$ ($\bar{\nu}_\mu \rightarrow \bar{\nu}_e$) transition and correspondingly a suppression (enhancement) of the $\nu_\mu \rightarrow \nu_\tau$ ($\bar{\nu}_\mu \rightarrow \bar{\nu}_\tau$) transition. The absolute size of $\Delta P = P_{mat} - P_{vac}$ is similar in both $\nu_\mu \rightarrow \nu_e$ and $\nu_\mu \rightarrow \nu_\tau$ oscillation, but in this second case the effect is much more difficult to detect, and less important to consider, because it represents a small correction to a probability of order unity.

Looking at fig. 10 and fig. 11 it is possible to observe that the matter effects are small both for large and small E_ν and most important in an intermediate energy. This is true in general and can be easily understood qualitatively. We can in fact consider three energy regions:

1. Large E_ν (or more precisely $E_\nu \gg \varepsilon_0$). In this region the oscillation length is much longer than the pathlength L ($L/\lambda_0(E_\nu) = \varepsilon_0/2E_\nu$), and therefore $P_{mat} \simeq P_{vac}$ for the reasons described in section 5.1.

For the existing long baseline projects, neutrinos with energy close to the MSW resonance ($E_\nu \sim \varepsilon_m$) belong to this region since $\varepsilon_m/\varepsilon_0$ is large, therefore the presence of matter does not result in large visible effects for neutrinos at the resonance, even if the effective masses and mixing are very different from the vacuum values.

2. Small E_ν (or more precisely $E_\nu \ll \varepsilon_m$). In this region the effective masses and mixing of neutrinos in matter are close to the vacuum values ($|x| = E_\nu/\varepsilon_m \ll 1$) and again one has $P_{mat} \simeq P_{vac}$.
3. Intermediate E_ν . In this region the neutrino energy is not much smaller than ε_m and it is not much larger than ε_0 . The first condition is needed to have significant modifications of on the effective masses and mixing, the second one to have a sufficiently large L/λ_0 . For the projected long baseline beams the two conditions can never be fully satisfied at the same time (because $\varepsilon_0/\varepsilon_m \leq 0.125$ and this is why the matter effects never produce very important effects. When the neutrino energy is $E_\nu \sim \varepsilon_0$ the conditions required to have significant matter effects are best satisfied, and this is where the matter effects manifest themselves most clearly.

Figures 10 and 11 have been calculated for a specific value of Δm^2 , but they describe oscillations also for an arbitrary value of Δm^2 . In fact the oscillation probabilities, for any distribution of matter along the neutrino path, are a function of $E_\nu/\Delta m^2$, and the figures be considered as valid for different values of Δm^2 simply rescaling the neutrino energy (for negative Δm^2 the probabilities for neutrinos and antineutrinos have to be interchanged). It remains to discuss matter effects for different neutrino mixings. This is illustrated in fig. 12 that describes the transition probability $P(\nu_\mu \rightarrow \nu_e)$ for the Fermilab to Soudan and CERN to Gran Sasso projects for an arbitrary value of Δm^2 and for all allowed possible mixings. In the figure we plot the probability $P(\nu_\mu \rightarrow \nu_e)$ divided by $4p_{e3}p_{\mu 3}$ (that is the amplitude of the oscillation probability in vacuum) as a function of

E_ν/ε_0 for neutrinos that have traveled a distance $L = 730$ km in vacuum (solid line) or in matter with constant density $\rho = 2.8$ g cm $^{-3}$ (dashed line for neutrinos, dot-dashed line for antineutrinos). All curves are valid for all values of $p_{\mu 3}$, and all positive values of Δm^2 (for $\Delta m^2 < 0$ the curve of ν and $\bar{\nu}$ have to be interchanged). The probability has been calculated for three values of the mixing $p_{e3} = \sin^2 \theta = 0.03, 0.02$ and 0.01 . The three curves for vacuum oscillations, are identical. The curves calculated taking into account the matter effects are very close to each other, and for $p_{e3} \rightarrow 0$ they tend to an asymptotic constant form. This can be simply understood observing that the $\nu\mu \rightarrow \nu_e$ (or $\bar{\nu}_\mu \rightarrow \bar{\nu}_e$) probability can be written as:

$$P_{\nu_\mu \rightarrow \nu_e}(E_\nu) = \frac{4 p_{\mu 3} p_{e3}}{F(x)} \sin^2 \left[\frac{\Delta m^2 \sqrt{F(x)} L}{4 E_\nu} \right], \quad (42)$$

where $x = \pm E_\nu/\varepsilon_m$ (the plus (minus) sign is for ν 's ($\bar{\nu}$'s)), and $F(x) = \sin^2 2\theta + (x - \cos 2\theta)^2$. When $p_{e3} = \sin^2 \theta$ is small (as indicated by the combined analysis of Chooz and Super-Kamiokande), $F(x)$ can be well approximated as $F(x) \simeq (1 - x)^2$, and the ratio $P(\nu_\mu \rightarrow \nu_e)/p_{e3}$ becomes independent from p_{e3} :

$$\frac{P_{\nu_\mu \rightarrow \nu_e}(E_\nu)}{4 p_{e3} p_{\mu 3}} \simeq \frac{1}{(1 - x)^2} \sin^2 \left[\frac{\pi}{2} \frac{\varepsilon_0 (1 - x)}{E_\nu} \right] \quad (43)$$

The main effect of matter on $P(\nu_\mu \rightarrow \nu_e)$ is an enhancement or suppression of the probability at the first maximum $P_{\nu(\bar{\nu})}^*$:

$$P_{\nu(\bar{\nu})}^* \simeq P_{vac}^* \left[1 \mp \frac{\varepsilon_0}{\varepsilon_m} \right]^{-2} \quad (44)$$

where $P_{vac}^* = 4 p_{\mu 3} p_{e3}$. The minus (plus) sign refers to ν 's ($\bar{\nu}$'s) for positive Δm^2 or viceversa for negative Δm^2 . The matter effects result also in a displacement of the energy $E_{\nu(\bar{\nu})}^*$ of the first maximum. Numerically (assuming $\Delta m^2 > 0$) for the Fermilab and CERN project ($L = 730$ km) one has:

$$P_\nu^* \simeq P_{vac}^* \cdot 1.26, \quad P_{\bar{\nu}}^* \simeq P_{vac}^* \cdot 0.76 \quad (45)$$

$$E_\nu^* \simeq \varepsilon_0 \cdot 0.92, \quad E_{\bar{\nu}}^* \simeq \varepsilon_0 \cdot 1.07 \quad (46)$$

For the K2K project ($L = 250$ km) one finds:

$$P_\nu^* \simeq P_{vac}^* \cdot 1.09, \quad P_{\bar{\nu}}^* \simeq P_{vac}^* \cdot 0.92 \quad (47)$$

$$E_\nu^* \simeq \varepsilon_0 \cdot 0.98, \quad E_{\bar{\nu}}^* \simeq \varepsilon_0 \cdot 1.02 \quad (48)$$

7 Discussion and conclusions

The effect of matter on neutrino oscillations in the projected long-baseline neutrino beams is small but detectable, especially for the longer pathlength and higher intensity Fermilab to Soudan and CERN to Gran Sasso beams.

In these experiments, assuming Δm^2 is positive, the effect of matter will manifest itself as an approximately 25% enhancement (suppression) of the $\nu_\mu \rightarrow \nu_e$ ($\bar{\nu}_\mu \rightarrow \bar{\nu}_e$) probability in the crucial region of the first maximum. The energy E_ν where the probability has the first maximum will also be lower (higher) than in vacuum by approximately 7%. In the shorter pathlength K2K project the matter effects will result in smaller effects: a 9% enhancement of the probability and a 2% displacement of the energy of the first maximum.

It is interesting to observe that the detectable effects of matter on the oscillations are most important not when E_ν is close to the MSW resonance, but at lower energy when the modifications induced by matter on the neutrino effective masses and mixing are smaller, but when the oscillations can develop because of a shorter oscillation length (comparable with L) and the modifications of the oscillation parameters can produce visible effects.

If Δm^2 , in contrast with the expectations, is negative, then the effects of matter on neutrinos and anti-neutrinos are reversed. This is perhaps the most interesting effect, because it provides a method to measure the sign of Δm^2 resolving the existing ambiguity. In order to do this one needs to produce (during different periods of data taking) beams of both neutrinos and anti-neutrinos inverting the polarity of the focusing system downstream of the target region, and to detect both $\nu_\mu \rightarrow \nu_e$ and $\bar{\nu}_\mu \rightarrow \bar{\nu}_e$ transitions, measuring the oscillation probabilities for energies $E_\nu \sim \varepsilon_0$. The ratio $P(\nu_\mu \rightarrow \nu_e)/P(\bar{\nu}_\mu \rightarrow \bar{\nu}_e)$ can have only two possible values (approximately 1.64 or 0.61 for the Fermilab and CERN projects, 1.18 or 0.85 for the K2K project) depending on the sign (positive or negative) of Δm^2 .

Acknowledgments

I would like to thank Maurizio Lusignoli and Giuseppe Battistoni for discussions and encouragement.

References

- [1] Y. Fukuda et al (Super-Kamiokande collaboration), Phys.Rev.Lett. **81**, 1562 (1998) (also hep-ex/9807003).
- [2] Y.Suzuki (for the Super-Kamiokande collaboration) in Proceedings of the 17th International Workshop on Weak Interactions and Neutrinos, WIN99 Cape Town (South Africa) January 1999.
- [3] Kamiokande collaboration, K.S. Hirata et al, Phys. Lett. B **205**, 416 (1988); Phys. Lett. B **280**, 146 (1992); Y. Fukuda et al, Phys. Lett. B **335**, 237 (1994).
- [4] IMB collaboration, D. Casper et al, Phys. Rev. Lett. **66**, 2561 (1991); IMB collaboration, R. Becker-Szendy et al, Phys. Rev. D **46**, 3720 (1992).
- [5] Soudan 2 Collaboration, W.W.M. Allison et al, hep-ex/9901024 (1999), to be published in Phys. Lett. B.
- [6] M. Ambrosio *et al.*, (MACRO collaboration) Phys. Lett. B **434**, 451 (1998) (also hep-ex/9807005); F. Ronga (for the MACRO collaboration), hep-ex/9810008, to appear in the proceedings of XVIII International Conference on Neutrino Physics and Astrophysics (Neutrino'98), Takayama, Japan, 4-9 June, 1998.
- [7] E. Akhmedov, P. Lipari and M. Lusignoli Phys. Lett. B **300**, 128, (1993) (also hep-ph/9211320); P. Lipari and M. Lusignoli, Phys. Rev. D **58**, 073005 (1998) (also hep-ph/9803440).
- [8] P. Lipari and M. Lusignoli, accepted for publication in Phys.Rev. D (1999) (also hep-ph/9801350).
- [9] A. Suzuki (for the Kamland collaboration) in Proceedings of the VIII International Workshop on Neutrino Telescopes, Venezia, february 1999; available at <http://axpd24.pd.infn.it/conference/>
- [10] M. Apollonio et al, Phys. Lett. B **240**, 397 (1998).
- [11] G.L. Fogli, E. Lisi, A. Marrone and G. Scioscia Phys. Rev. D **559**, 033001 (1999), also hep-ph/98082.
- [12] E. Kh. Akhmedov, A. Dighe, P. Lipari and A. Yu. Smirnov Nucl.Phys. B **542**, 3 (1999).
- [13] M. Chizhov, M. Maris and S.T. Petcov, SISSA report 53/98/EP (1998) (also hep-ph/9810501).
- [14] For updated information on the status of the LBL projects see the web pages of "The Neutrino Oscillation Industry" at: <http://www.hep.anl.gov/NDK/HyperText/-nuindustry.html>.

- [15] H.Sobel (for the Super-Kamiokande collaboration) in Proceedings of the VIII International Workshop on Neutrino Telescopes, Venezia, february 1999; available at <http://axpd24.pd.infn.it/conference/>
- [16] R.Bernstein, in Proceedings of the VIII International Workshop on Neutrino Telescopes, Venezia, february 1999; available at <http://axpd24.pd.infn.it/conference/>.
- [17] C. Acquistapace et al., “The CERN Neutrino beam to Gran Sasso (NGS)” preprint INFN/AE-98/05 (1998).
- [18] L. Wolfenstein, Phys. Rev. D **17**, 2369 (1978); Phys. Rev. D **20**, 2634 (1979); Mikheyev and A. Smirnov, Sov.J.Nucl.Phys. **42**, 913 (1986).
- [19] J.Pantaleone Phys. Lett. B **292**, 201 (1992); Phys. Rev. D **49**, 2152 (1994); Phys. Rev. Lett. **81** 5060, (1998).
- [20] G. L. Fogli, E. Lisi and G. Scioscia Rev. D **52**, 5334, (1995); G.L.Fogli, E.Lisi, D.Montanino, and G.Scioscia, Phys. Rev. D **55** 4385, (1997);
- [21] C.Y. Cardall, and G.M. Fuller Phys. Rev. D **53**, 4421 (1996).
- [22] J.N. Bahcall, P.I. Krastev and A.Yu. Smirnov Phys. Rev. D **58**, 096016 (1998) (also hep-ph/980721) and references therein.
- [23] O.L.G. Peres and A.Yu.Smirnov hep-ph/9902312 (1999).
- [24] C. Giunti, C.W. Kim, U.W. Lee and V.A. Naumov, hep-ph/9902261 (1999).

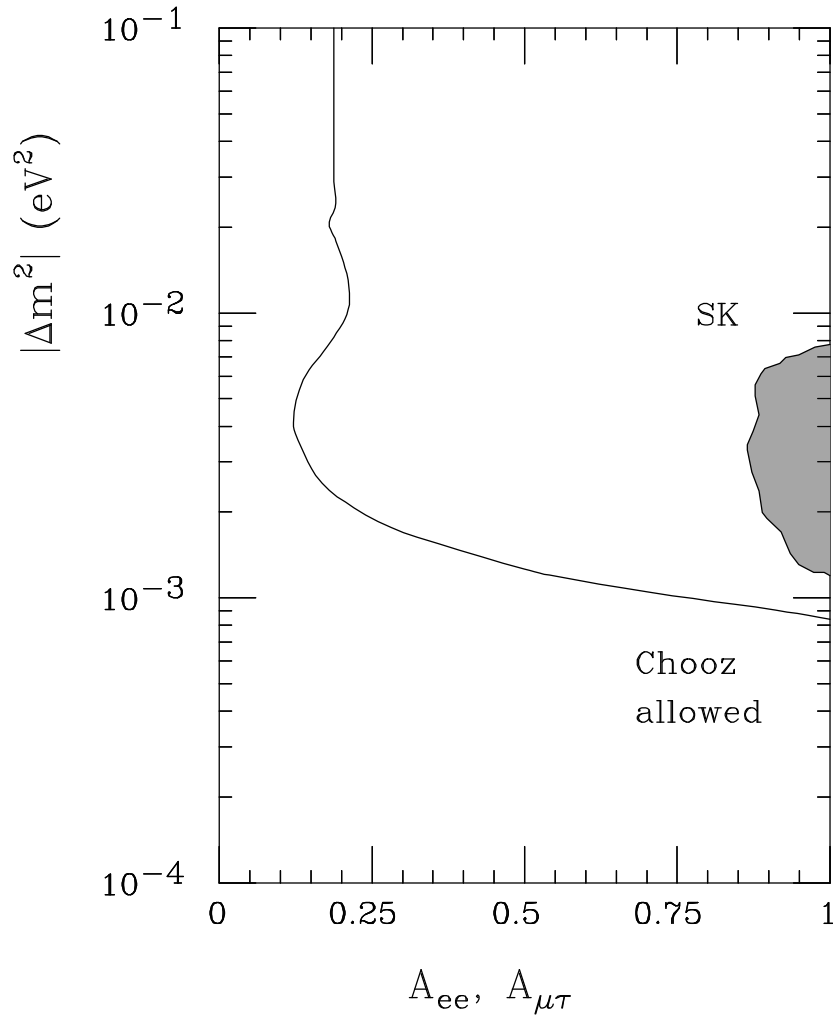


Figure 1: Limits on $\nu_\mu \rightarrow \nu_\tau$ and $\nu_e \rightarrow \nu_e$ transitions obtained by the Super-Kamiokande and Chooz experiments.

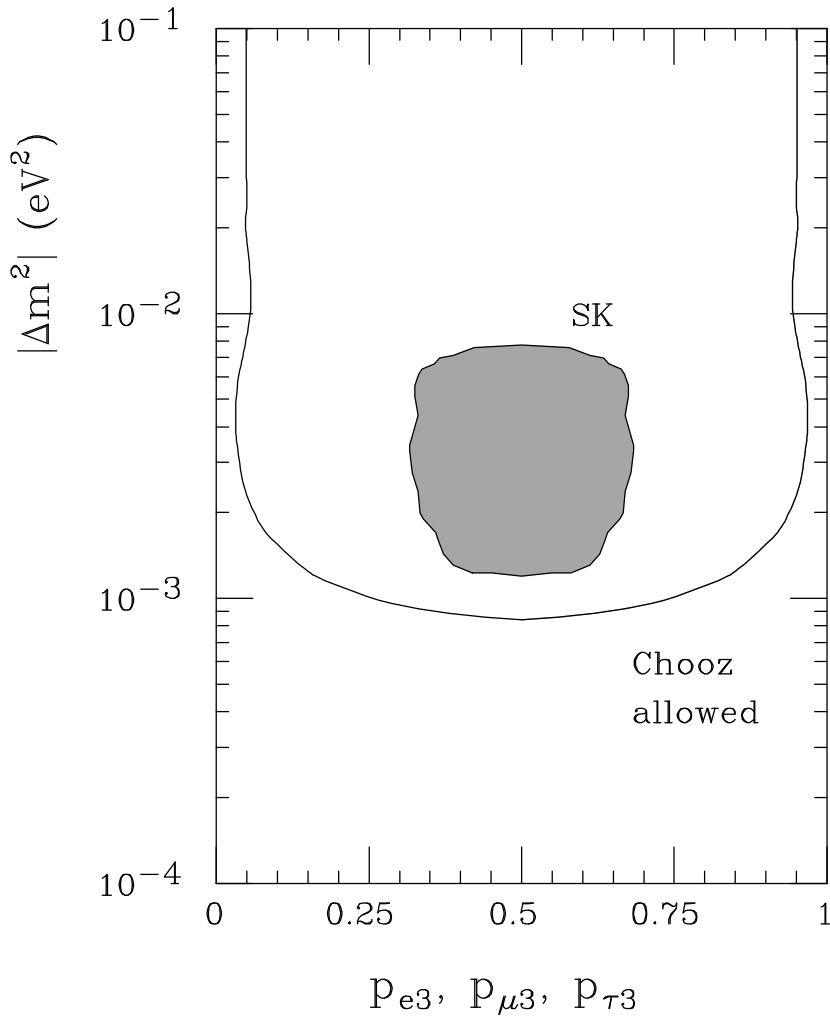


Figure 2: Limits on the flavor content $p_{\alpha 3} = |\langle \nu_{\alpha} | \nu_3 \rangle|^2$ of the neutrino state $|\nu_3\rangle$ obtained from the results of the SK and Chooz experiment. The SK results give an allowed interval for $p_{\mu 3}$ and $p_{\tau 3}$; the Chooz results give an allowed interval for $p_{e 3}$.

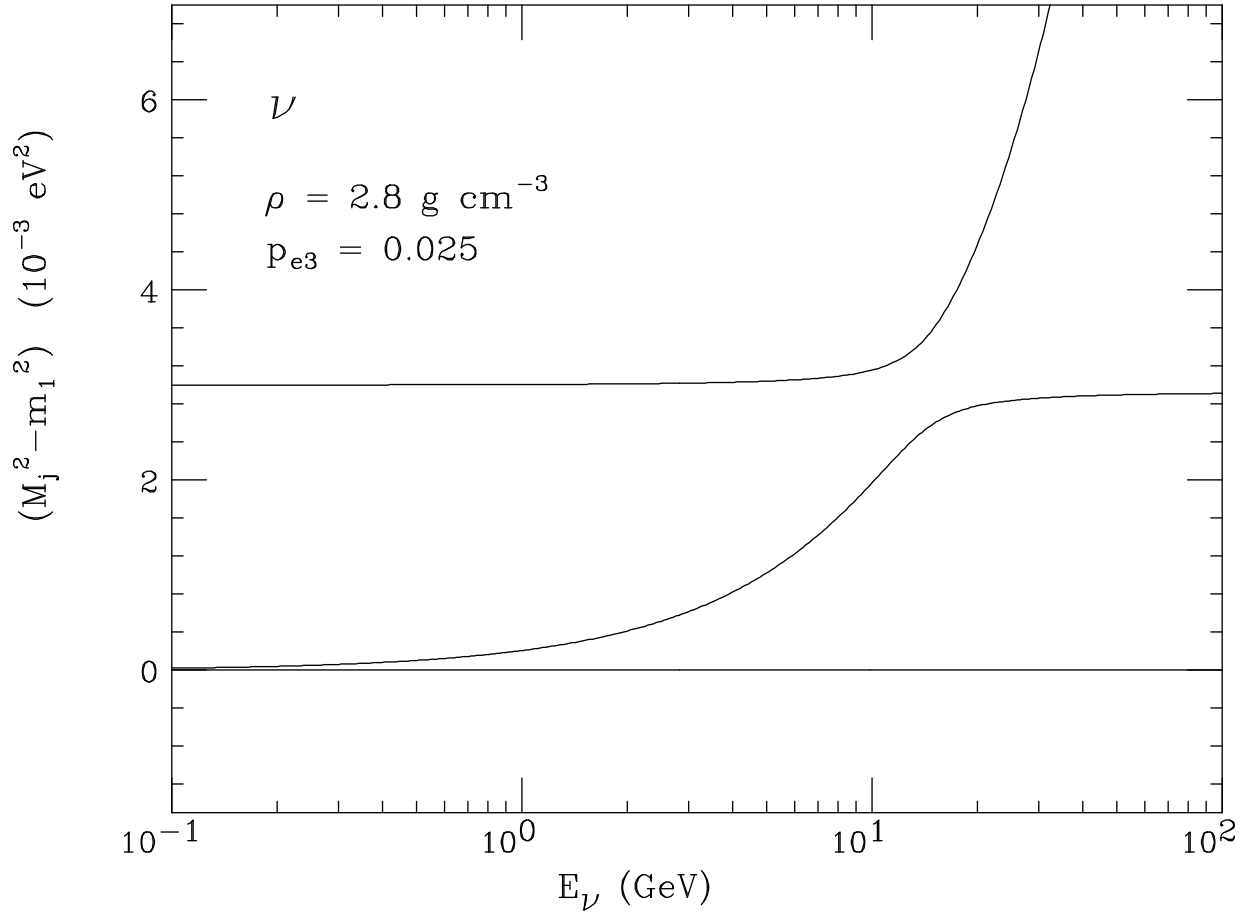


Figure 3: Effective mass eigenvalues for neutrinos propagating in matter with density $\rho = 2.8 \text{ g cm}^{-3}$ (and electron fraction $Y_e = n_e/(n_p + n_n) = 1/2$) plotted as a function of E_ν . The neutrino masses are $m_1^2 = m_2^2$, and $m_3^2 = m_1^2 + 3 \cdot 10^{-3} \text{ eV}^2$. The neutrino state $|\nu_3\rangle$ as a probability $p_{e3} = \sin^2 \theta = 0.025$ of having electron flavor.

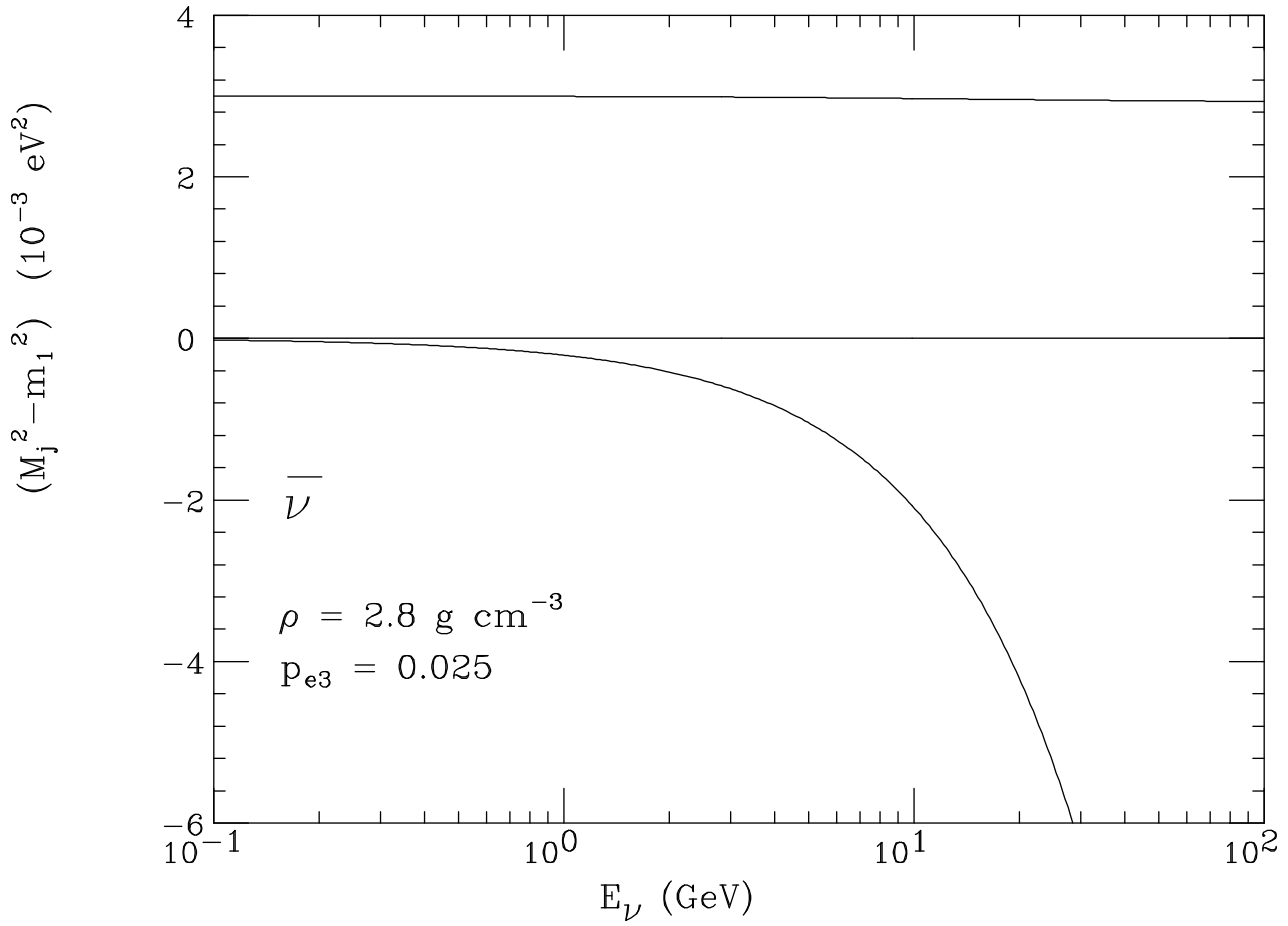


Figure 4: Effective mass eigenvalues of anti-neutrinos, propagating in matter with density $\rho = 2.8 \text{ g cm}^{-3}$. The neutrino masses and mixing are the same as in fig. 1.

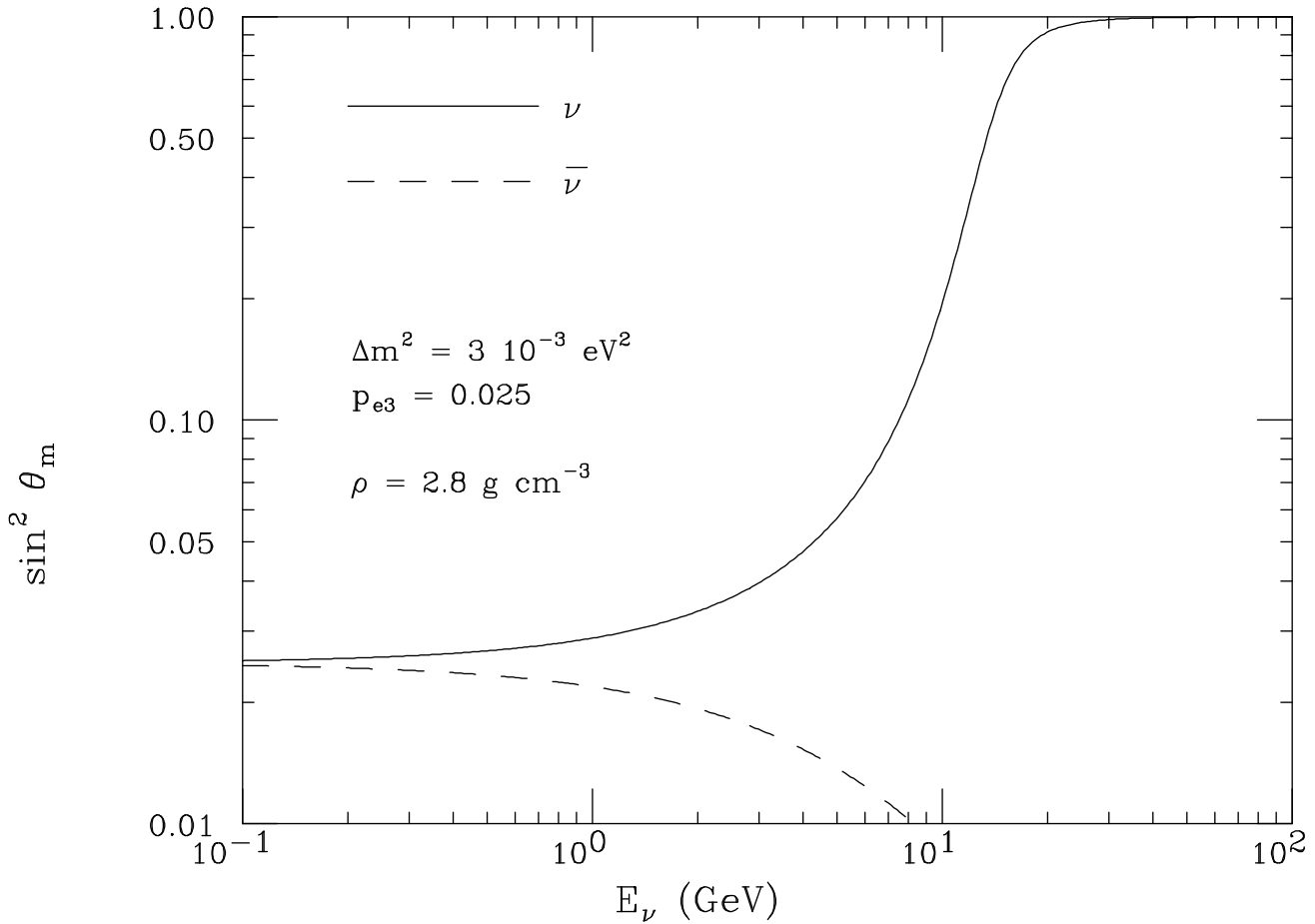


Figure 5: Value of $\sin^2 \theta_m$ plotted as a function of E_ν for neutrinos (solid line) and antineutrinos (dashed line) propagating in matter with density $\rho = 2.8 \text{ g cm}^{-3}$. In vacuum $p_{e3} = \sin^2 \theta = 0.025$. The neutrino masses are $m_1 = m_2$, $m_3^2 = m_1^2 + 3 \cdot 10^{-3} \text{ eV}^2$.

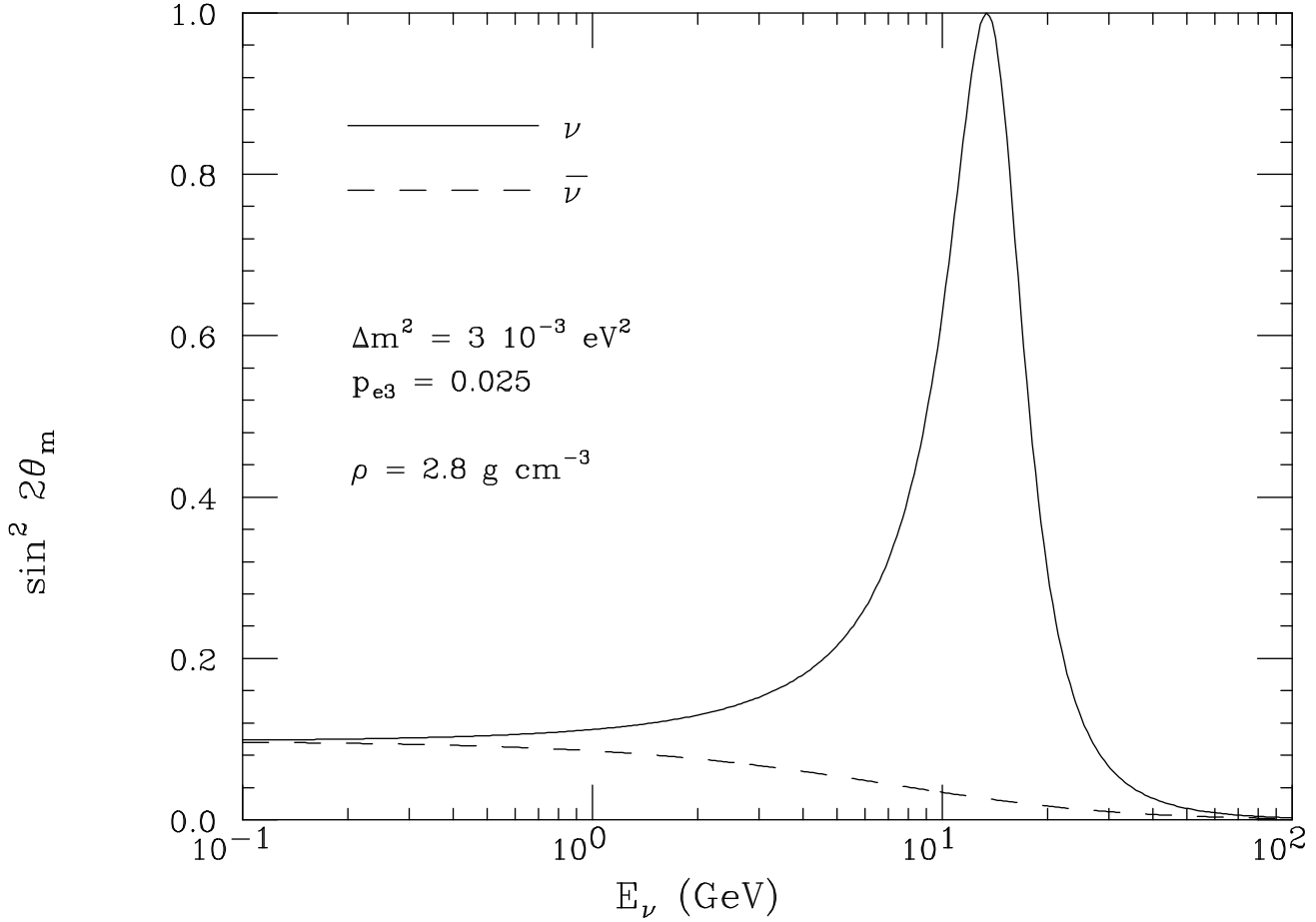


Figure 6: Value of $\sin^2 2\theta_m$ plotted as a function of E_ν for neutrinos (solid line) and antineutrinos (dashed line) propagating in matter with density $\rho = 2.8 \text{ g cm}^{-3}$. In vacuum $p_{e3} = \sin^2 \theta = 0.025$ ($\sin^2 2\theta = 0.0975$). The neutrino masses are $m_1 = m_2$, $m_3^2 = m_1^2 + 3 \cdot 10^{-3} \text{ eV}^2$.

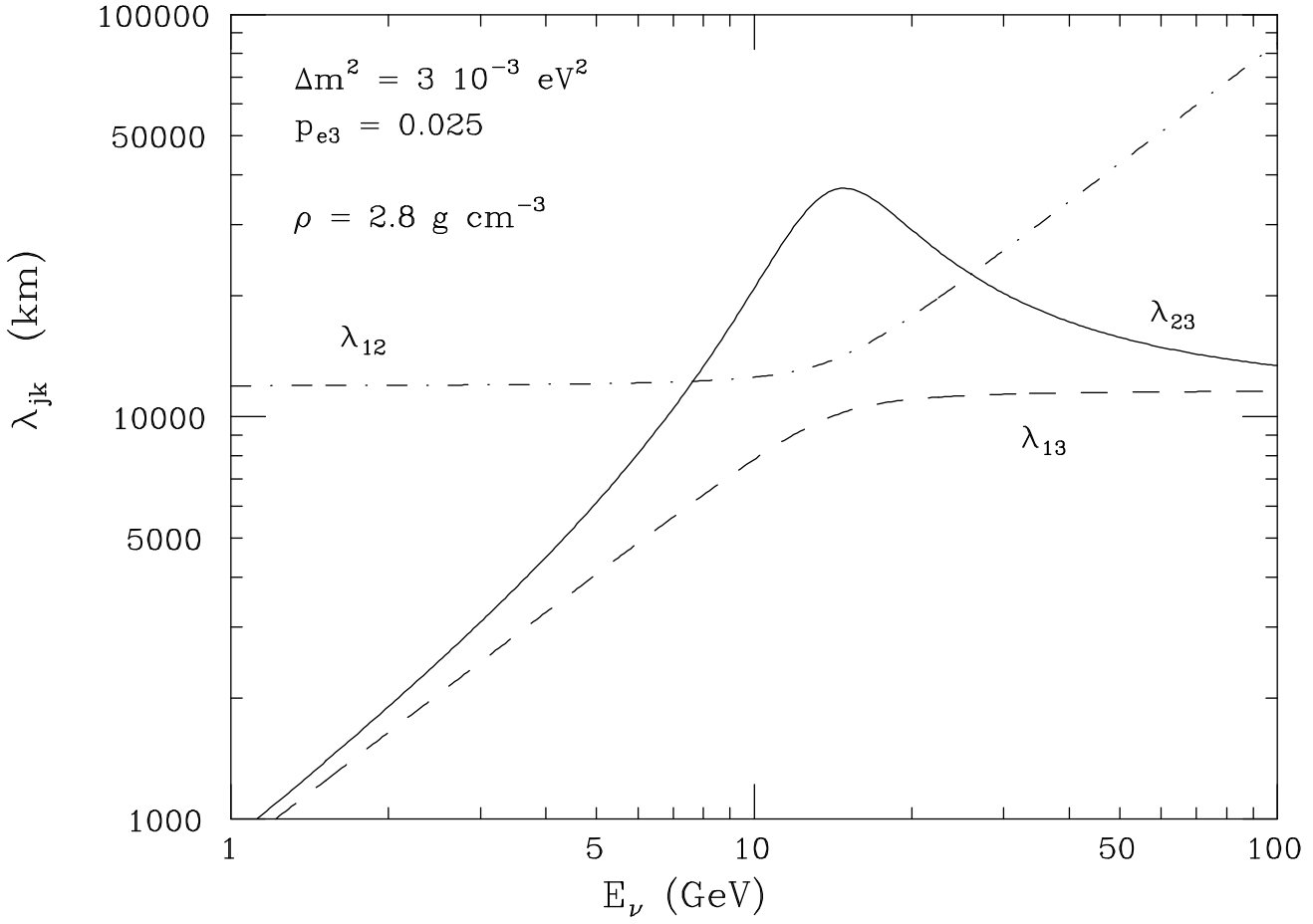


Figure 7: Oscillation lengths $\lambda_{jk} = 4\pi E_\nu / |M_j^2 - M_k^2|$ plotted as a function of E_ν for neutrinos traveling in matter of density $\rho = 2.8 \text{ g cm}^{-3}$. The neutrino masses are $m_1 = m_2$, $m_3^2 = m_1^2 + 3 \cdot 10^{-3} \text{ eV}^2$, the electron flavor content of the state $|\nu_3\rangle$ is $p_{e3} = \sin^2 \theta = 0.025$.

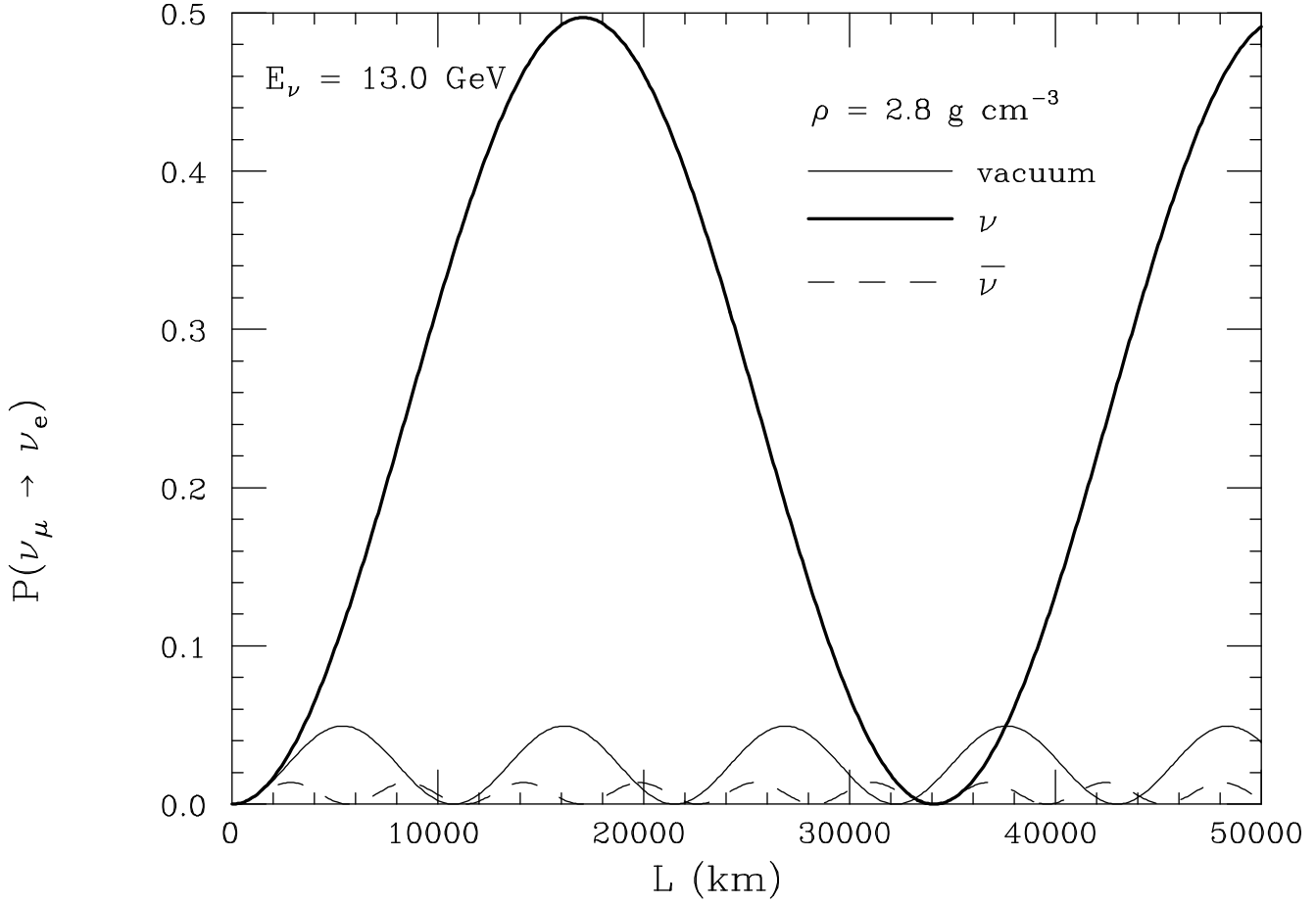


Figure 8: Transition probability $P(\nu_\mu \rightarrow \nu_e)$, plotted as a function of the distance L for neutrinos with a fixed energy $E_\nu = 13.0 \text{ GeV}$ traveling in vacuum (solid line) or in matter of constant matter with density $\rho = 2.8 \text{ g cm}^{-3}$ (thick solid line for neutrinos, dashed line for antineutrinos). The neutrino masses are $m_1 = m_2$, $m_3^2 = m_1^2 + 3 \cdot 10^{-3} \text{ eV}^2$. The mixing matrix in vacuum is determined by $p_{e3} = \sin^2 \theta = 0.025$ and $p_{\mu 3} = p_{\tau 3}$ ($\sin^2 \varphi = 0.5$). $E_\nu = 13.0 \text{ GeV}$ is close to the resonance energy for the density and parameter values considered.

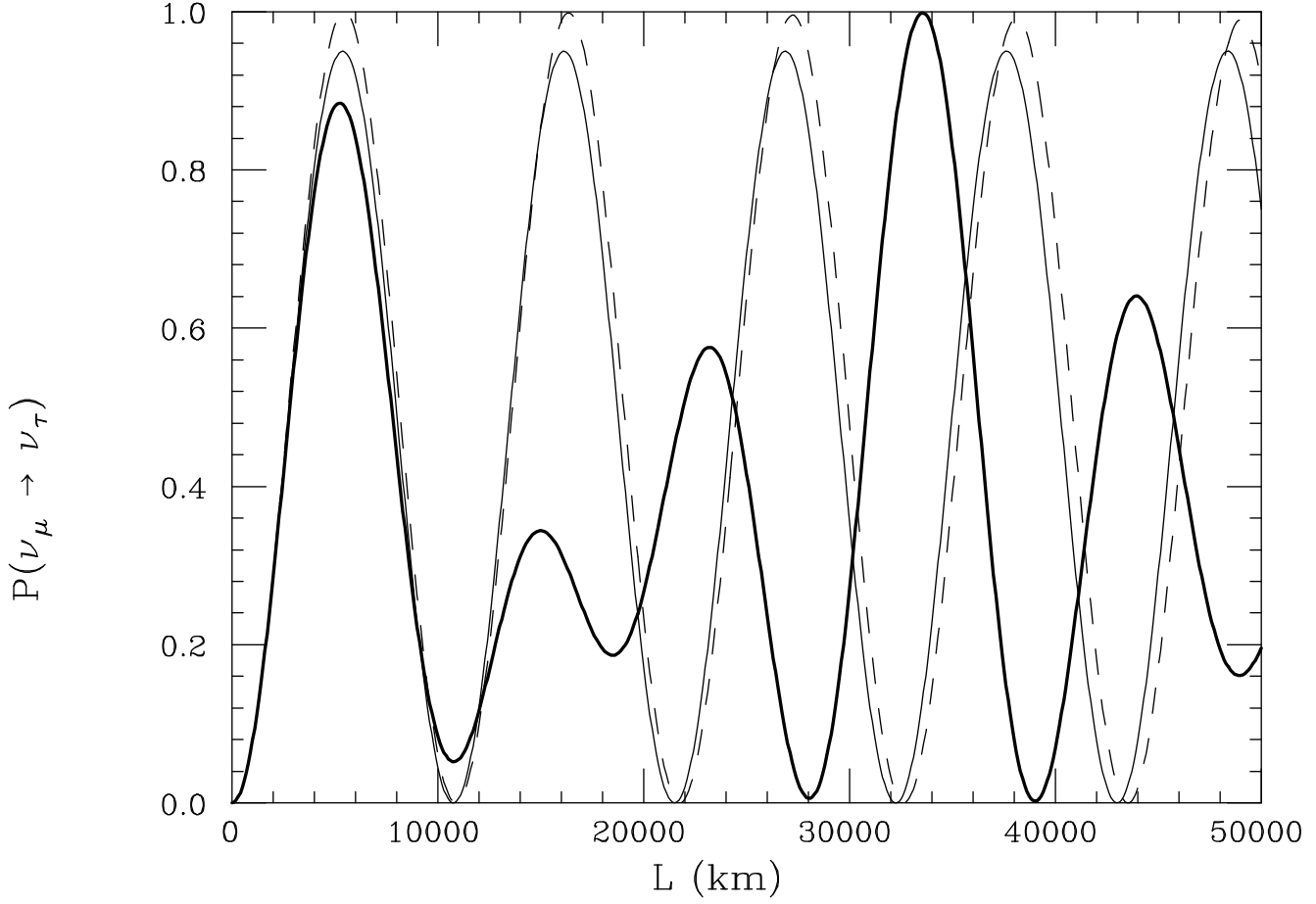


Figure 9: Transition probability $P(\nu_\mu \rightarrow \nu_\tau)$, plotted as a function of the distance L for neutrinos with a fixed energy $E_\nu = 13.0$ GeV traveling in vacuum (thin solid line) or in matter of constant matter with density $\rho = 2.8$ g cm $^{-3}$ (thick solid line for neutrinos, dashed line for antineutrinos). The neutrino masses are $m_1 = m_2$, $m_3^2 = m_1^2 + 3 \cdot 10^{-3}$ eV 2 . The mixing matrix in vacuum is determined by $p_{e3} = \sin^2 \theta = 0.025$ and $p_{\mu 3} = p_{\tau 3}$ ($\sin^2 \varphi = 0.5$). $E_\nu = 13.0$ GeV is close to the resonance energy for the density and parameter values considered.

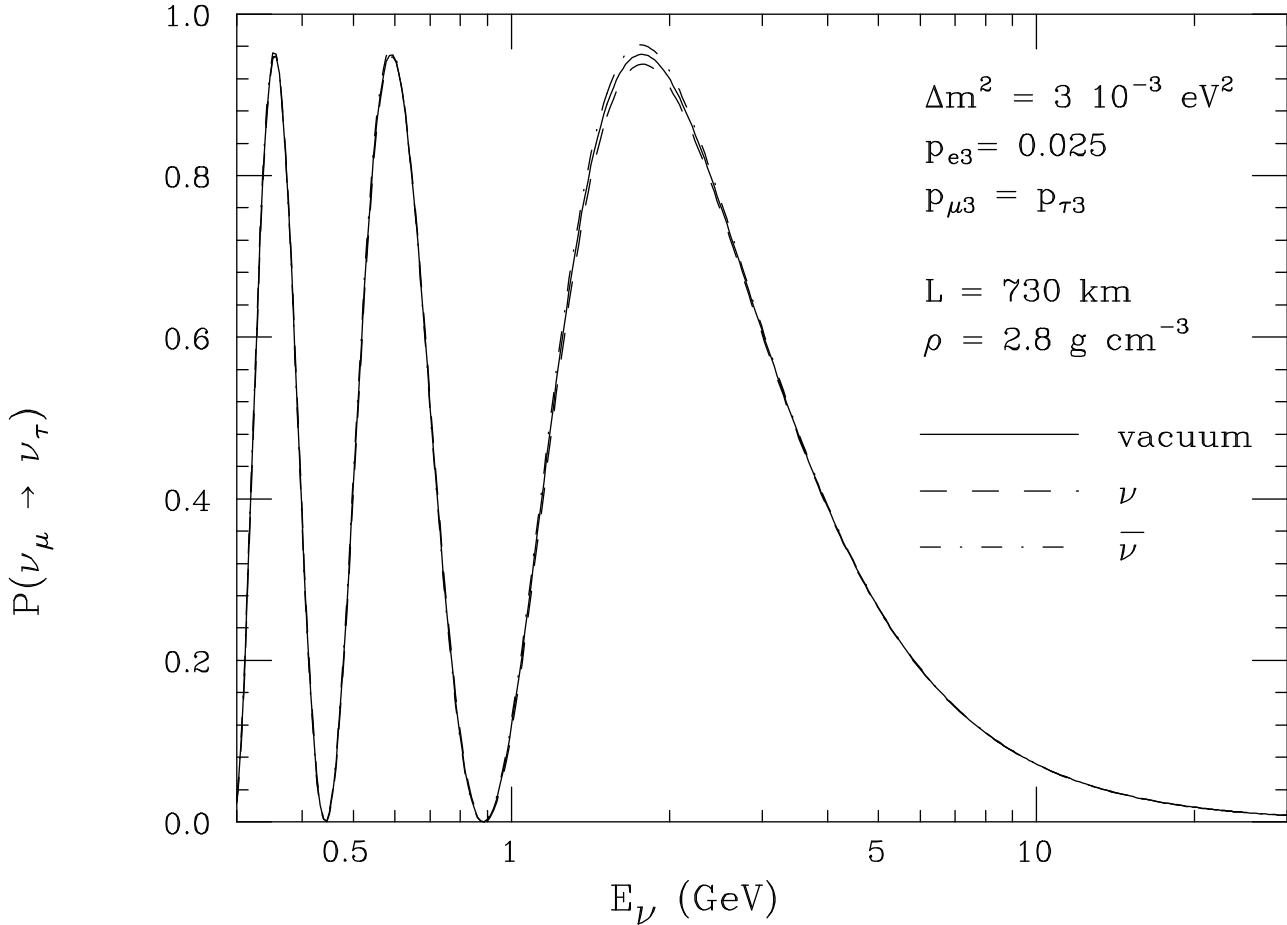


Figure 10: Transition probability $P(\nu_\mu \rightarrow \nu_\tau)$ plotted as a function of E_ν for neutrinos that have traveled a distance $L = 730 \text{ km}$ in vacuum (solid line) or in matter with constant density $\rho = 2.8 \text{ g cm}^{-3}$ (dashed line for neutrinos, dot-dashed line for antineutrinos). The neutrino masses are $m_1 = m_2$, $m_3^2 = m_1^2 + 3 \cdot 10^{-3} \text{ eV}^2$. The mixing matrix in vacuum is determined by $p_{e3} = \sin^2 \theta = 0.025$ and $p_{\mu 3} = p_{\tau 3}$ ($\sin^2 \varphi = 0.5$).

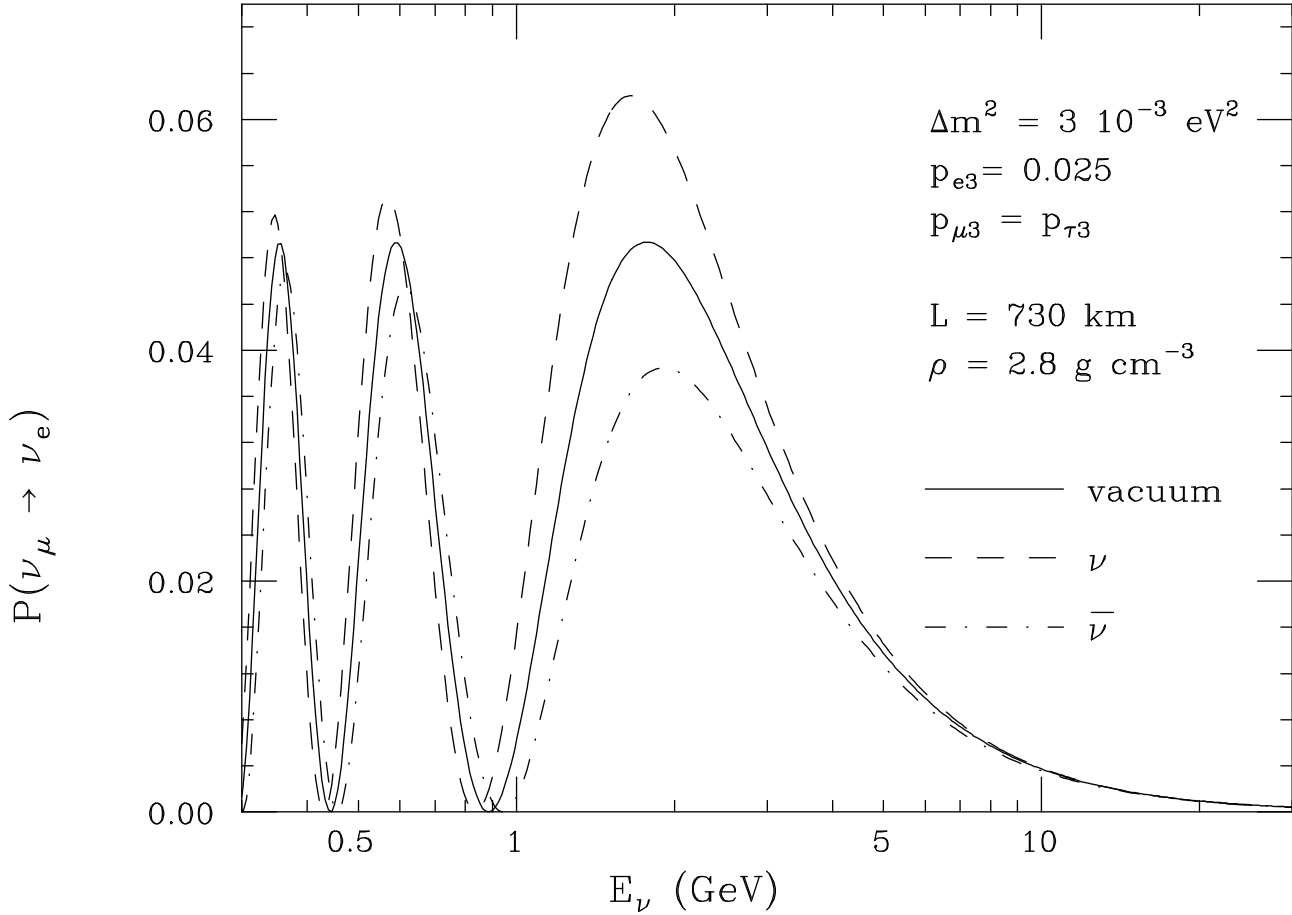


Figure 11: Transition probability $P(\nu_\mu \rightarrow \nu_e)$, plotted as a function of E_ν for neutrinos that have traveled a distance $L = 730$ km in vacuum (solid line) or in matter with constant density $\rho = 2.8 \text{ g cm}^{-3}$ (dashed line for neutrinos, dot-dashed line for antineutrinos). The neutrino masses are $m_1 = m_2$, $m_3^2 = m_1^2 + 3 \cdot 10^{-3} \text{ eV}^2$. The mixing matrix in vacuum is determined by $p_{e3} = \sin^2 \theta = 0.025$ and $p_{\mu 3} = p_{\tau 3}$ ($\sin^2 \varphi = 0.5$).

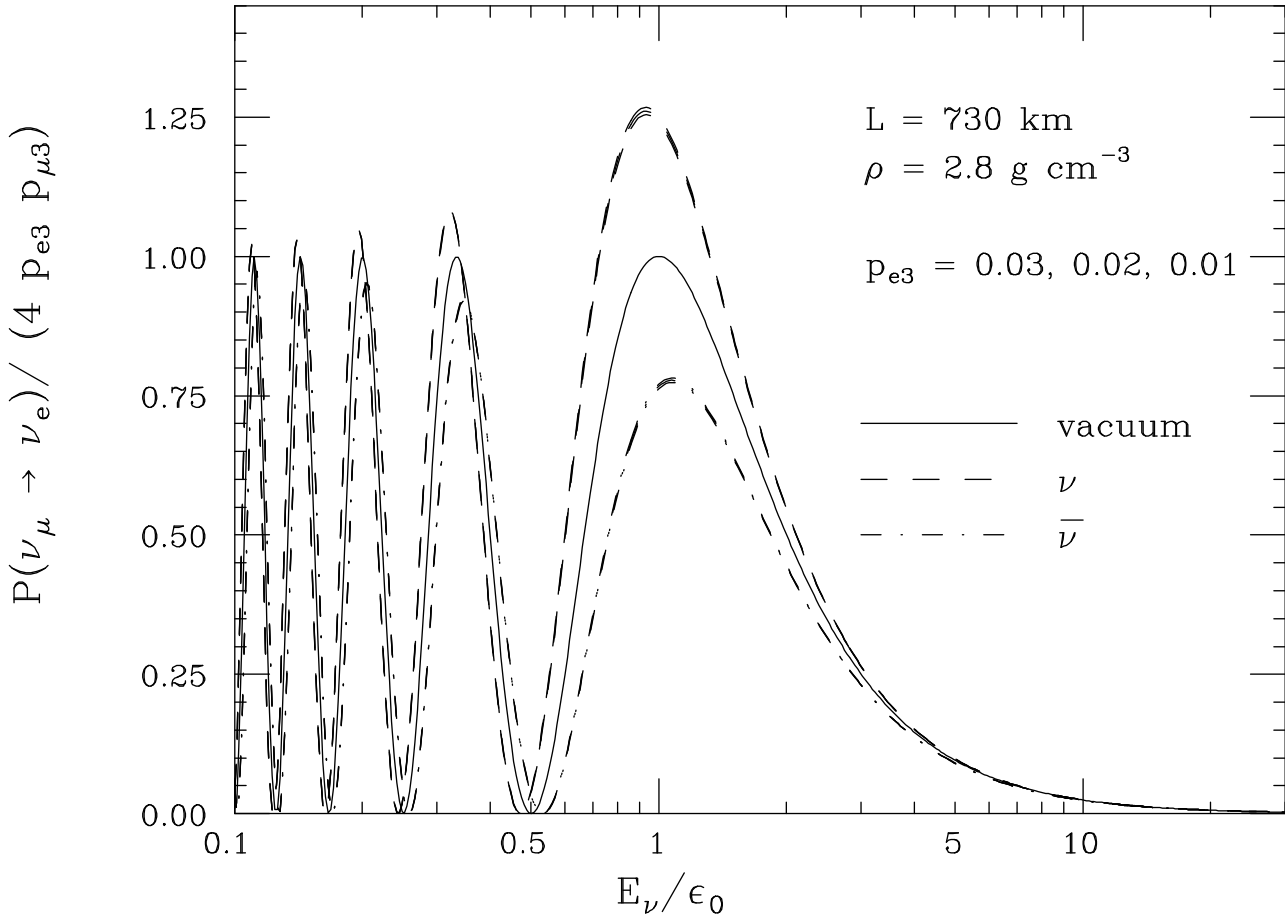


Figure 12: Transition probabilities $P(\nu_\mu \rightarrow \nu_e)$, plotted as a function of E_ν/ϵ_0 for neutrinos that have traveled a distance $L = 730 \text{ km}$ in vacuum (solid line) or in matter with constant density $\rho = 2.8 \text{ g cm}^{-3}$ (dashed line for neutrinos, dot-dashed line for antineutrinos). All curves are valid for all values of $p_{\mu 3}$ and all positive values of Δm^2 , for negative Δm^2 the neutrino and anti-neutrino curves have to be interchanged. The probability has been calculated for $p_{e3} = \sin^2 \theta = 0.03, 0.02$ and 0.01 . The three curves for vacuum oscillations, are identical, the curves calculated taking into account the matter effects are very close to each other.